

BULETINUL INSTITUTULUI POLITEHNIC DIN IAȘI
Publicat de
Universitatea Tehnică „Gheorghe Asachi” din Iași
Volumul 64 (68), Numărul 4, 2018
Secția
ELECTROTEHNICĂ. ENERGETICĂ. ELECTRONICĂ

PERMANENT MAGNET-ASSISTED SYNCHRONOUS RELUCTANCE MACHINE IN ELECTRIC GENERATOR OPERATING MODE

BY

MIRCEA M. RĂDULESCU* and HILDA FÜLÖP

Technical University of Cluj-Napoca,
Department of Electric Machines and Drives

Received: September 28, 2018

Accepted for publication: October 31, 2018

Abstract. This paper proposes the ferrite magnet-assisted synchronous reluctance machine topologies for use as direct-driven generators in low-speed micro-wind power applications. The ferrite magnet-assisted synchronous reluctance generator (FMASRG) consists of a stator core hosting three-phase distributed winding, and a transversally-laminated rotor having multilayer flux-barriers with embedded FMs in flux-concentration arrangement. Analytical model based on d - and q -axis magnetic circuit equivalent schemes is developed for the preliminary electromagnetic design. Finite-element magnetic field analyses are employed for evaluation of FMASRG design results and of output performances by dynamic simulations.

Keywords: ferrite magnet-assisted synchronous reluctance generator; electromagnetic design; finite-element magnetic field analysis; dynamic simulation.

1. Introduction

The aim of the present paper is to investigate the feasibility of using ferrite magnet-assisted synchronous reluctance machine topologies for direct-drive micro-wind generator applications. The emphasis is on the design analysis

*Corresponding author: *e-mail*: Mircea.Radulescu@emd.utcluj.ro

of ferrite magnet-assisted synchronous reluctance generators (FMASRGs) having (i) the stator structure similar to synchronous machines with three-phase distributed winding, and (ii) the rotor built of conventional transverse laminations with stamped multilayer magnetic-flux barriers, having constant thicknesses along their spans and being filled with FMs in flux-concentration disposal. The electromagnetic torque developed by the FMASRG has reluctance torque, mutual (or FM-alignment) torque and cogging torque components (Fülöp *et al.*, 2017). The reluctance torque depends on the difference between d - and q -axis inductances, whereas the mutual torque depends on the amount of rotor FMs in the machine. Due to the high magnetic saliency of the rotor created by flux barriers, reluctance torque component is prevalent at low speeds. FM-rotor excitation is only needed as an additional contribute to the developed electromagnetic torque along with an improvement for the power factor. In its turn, the cogging torque is due to the interaction through the agency of the magnetic field between the stator teeth and rotor FMs (Vagati *et al.*, 2014; Boazzo *et al.*, 2015). The paper is organized as follows. In Section 2, the electromagnetic modelling and design of two FMASRG topologies intended for use as low-speed electric generators in micro-wind power applications are approached. Section 3 is focused on finite-element field analyses and dynamic simulations for evaluation of design results and output performances for the proposed FMASRG topologies. Conclusions are drawn in the last section.

2. Electromagnetic Modelling and Design of FMASRGs

The analytical electromagnetic model of the FMASRGs is developed in the d, q synchronously rotating reference (Baek *et al.*, 2013). In the steady-state phasor diagram of the FMASRG mode of operation (Fig. 1), the q -axis is aligned with the rotor-FM magnetic flux, and the d -axis is aligned to the back-EMF E_{PM} , *i.e.* to the maximum permeance direction.

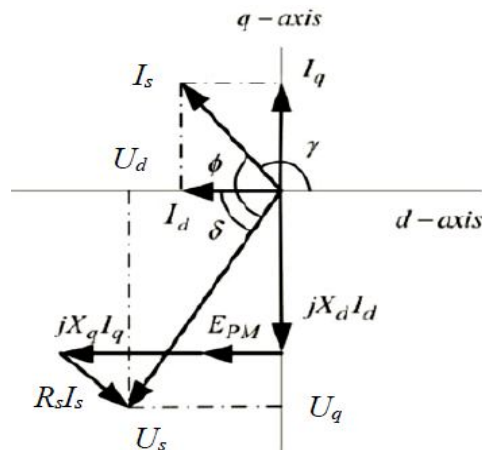


Fig. 1 – Steady-state phasor diagram of the FMASRG.

The available maximum output power can be controlled by the negative I_d and the positive I_q components of the current strength phasor. The angle δ between the current strength component I_d and the stator voltage phasor U_s denotes the torque angle, whereas γ stands for the current strength phasor angle and ϕ , for the power factor angle.

The two proposed FMASRG topologies have 8 poles and 12 poles on the rotor, respectively, with three layers of U-shaped flux barriers per pole whose lateral parts contain parallelipipedic FMs with tangential magnetization in flux-concentration disposal to increase the q -axis magnetic flux. The flux barriers create high rotor magnetic saliency thus making the reluctance torque dominant at low speeds, and also prevent magnetic saturation along the q -axis of the rotor core.

Fig. 2 depicts the q -axis equivalent magnetic circuit corresponding to the first layer of rotor flux barrier sideways filled with a block-type FM. In Fig. 2, notations are f_{qrk} , for the k -th layer rotor-surface MMF potential, and r_{mk} , r_{gk} , for the k -th rotor cavity reluctance and for the k -th airgap segment reluctance, respectively. The rotor-FM flux Φ_m is oriented along the q -axis, and the magnetic circuit is analyzed with the stator MMF sources removed.

The magnetic flux flowing through the airgap in front of the rotor portion bordered by the first magnetic flux barrier is referred to as Φ_{g1} , the airgap flux flowing between the first and the second flux-barrier ends is referred to as Φ_{g2} , and the magnetic flux Φ_b stands for the FM leakage flux flowing through the saturated iron ribs (near the airgap) at the end of each flux barrier.

Fig. 3 illustrates the nonlinear d -axis equivalent magnetic circuit with the rotor core saturated by the magnetic flux flowing along the narrow sections separated by the flux-barrier layers. In this magnetic circuit, the saturable reluctances of the rotor-core flux paths, r_{ryk} , as well as of the stator teeth and yoke segments, r_{dk} , r_{syk} , are nonlinear functions based on the $B-H$ characteristic of core material; f_{dk} represents the stator MMF source for the k -th segment.

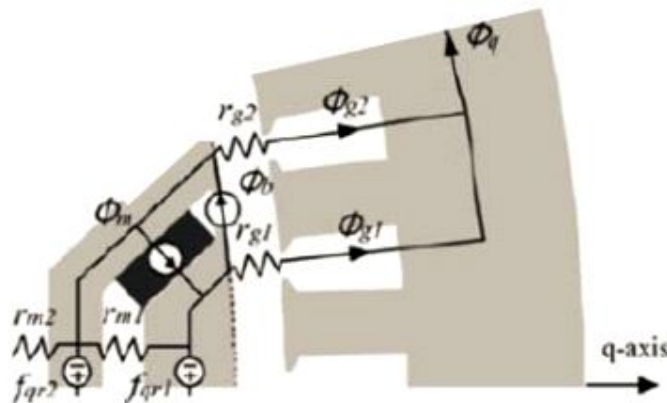


Fig. 2 – FMASRG linear q -axis equivalent magnetic circuit corresponding to the first layer of rotor flux barrier.

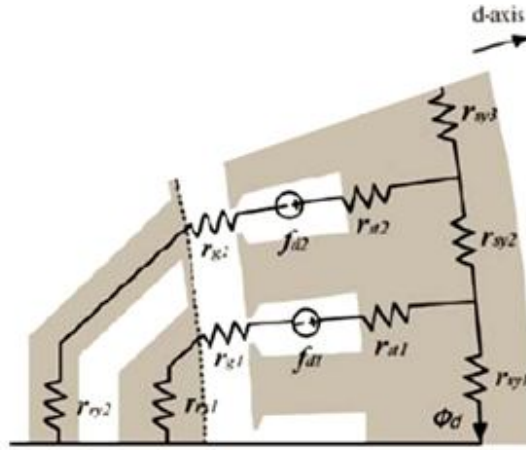


Fig. 3 – FMSRG nonlinear d -axis equivalent magnetic circuit for the rotor-core magnetic paths bordering the first flux barrier.

The stator of both proposed FMSR micro-wind generators accommodates a three-phase two-layer winding distributed into 36 slots with the presumed advantages of low back-EMF harmonics and electromagnetic torque ripple. The outer stator diameter is set to 190 mm.

It is to be noted that the opening angles of the rotor-core U-shaped flux barriers are provided acute enough to prevent inter-polar crossing, and the flux barriers as well as the corresponding iron magnetic flux-path segments have the same width along tangential and radial directions. The main design data for the two proposed FMSRGs, resulting from the given specifications and the analytical electromagnetic model, are presented in Table 1.

Table 1
Main Design Data of the Proposed Fmsrgs

Design data	Value
Number of stator phases	3
Number of stator slots	36
Number of rotor poles	12/8
Stator outer diameter, [mm]	190
Stator inner diameter, [mm]	115
Airgap radial length, [mm]	0.5
Rotor inner diameter (shaft diameter), [mm]	28.5
Number of rotor flux-barrier layers per pole	3
Axial stack length, [mm]	50

The preliminary design of the two proposed FMSRGs with cross-sectional main dimensions are shown in Figs. 4 and 5.

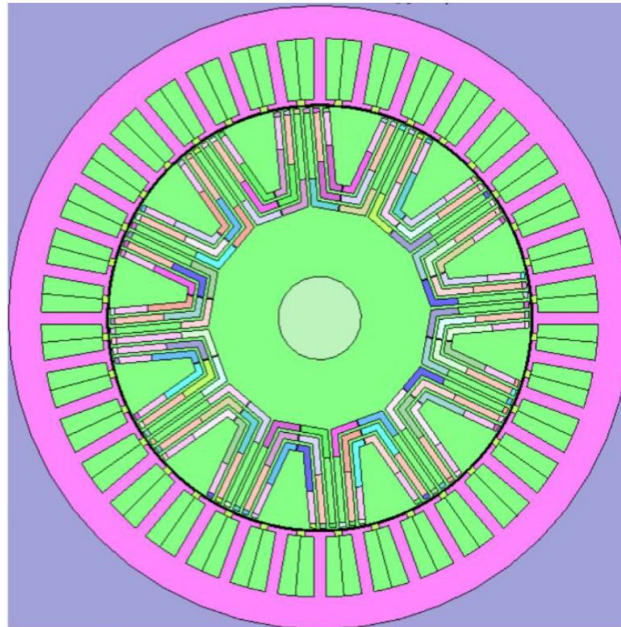


Fig. 4 – Cross-section of the preliminary design for the proposed 12-rotor-pole FMSRG.

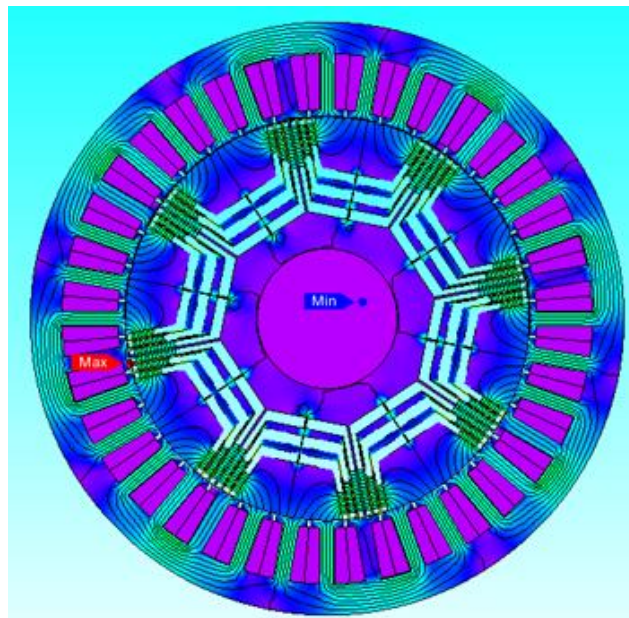


Fig. 5 – Cross-section of the preliminary design for the proposed 8-rotor-pole FMSRG with display of the rotor FM-created magnetic flux distribution.

3. Evaluation of FMSRGS Designs and Output Performances by Finite-Element-Based Field Analyses and Dynamic Simulations

The preliminary design evaluation for the proposed FMSRGS is conducted by time-stepped 2-D finite-element (FE) magnetic field analysis using the commercially-available software JMAG Designer.

At no-load (open stator-circuit) operation of the FMSRGS, there is no electric current in the stator winding, and the rotor-FMs placed on the sides of flux barriers and in flux-concentration arrangement are the only sources of magnetic flux in the machine. Rotor FM-created magnetic flux-line distribution and flux-density map from 2-D FE analyses of the FMSRGS designs are displayed in Figs. 6 and 7. It is proved that magnetic saturation concerns only the iron ribs (near the airgap) at the ends of rotor flux-barriers.

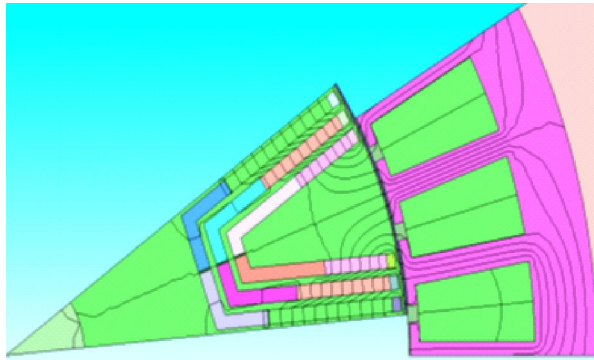


Fig. 6 – Rotor-pole FM-created magnetic flux-line distribution for the proposed 12-pole-rotor FMSRGS design.

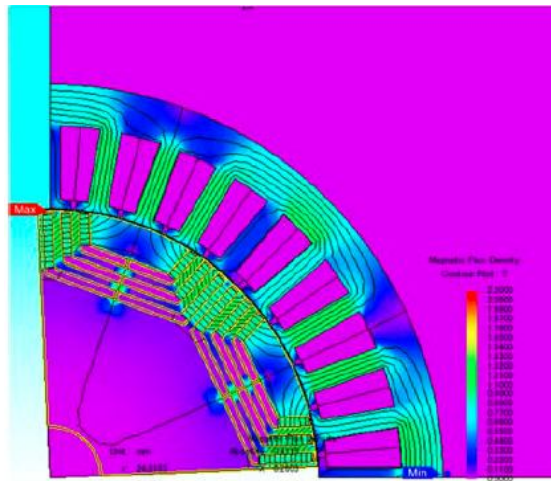


Fig. 7 – Rotor FM-created magnetic flux-density map and flux-line distribution for the proposed 8-pole-rotor FMSRGS design.

Figs. 8 and 9 show the FE-computed stator-phase back-EMFs induced by the rotor-FM flux linkage for 12-pole-rotor and 8-pole-rotor FMSRG topologies. It can be seen that the stator-phase back-EMF waveforms are quite sinusoidal in both cases.

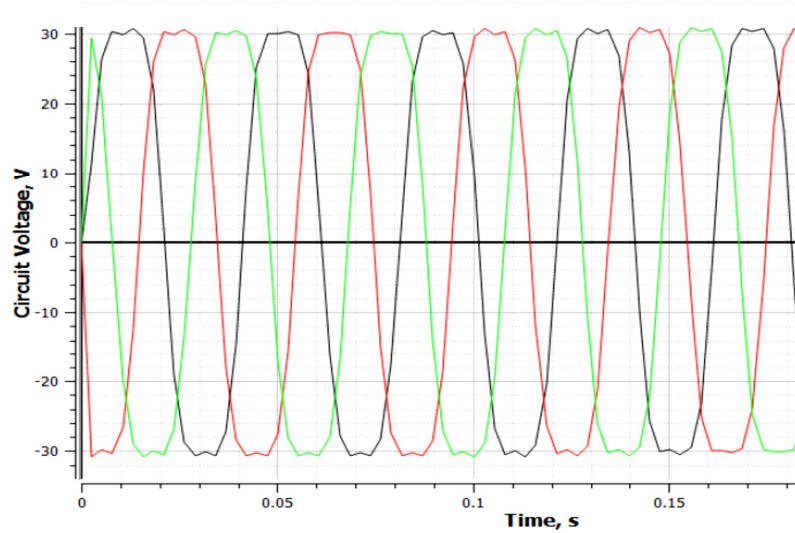


Fig. 8 – FE-computed stator-phase back-EMFs induced by rotor-FM flux linkage for the proposed 12-pole-rotor FMSRG.

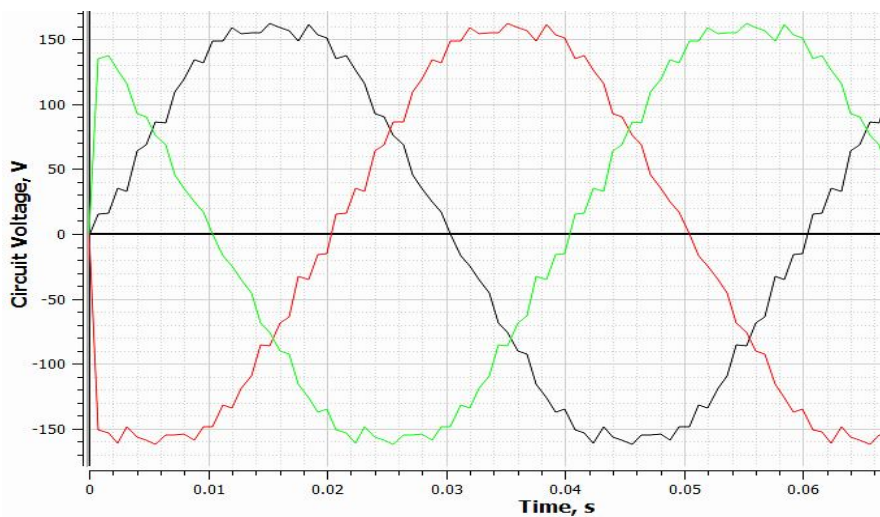


Fig. 9 – FE-computed stator-phase back-EMFs induced by rotor-FM flux linkage for the proposed 8-pole-rotor FMSRG.

In Fig. 10, the FE-computed cogging (or detent) torque waveform is presented. As the mean value of the cogging torque is null, it has no contribution to the net electromagnetic torque developed, instead it increases torque ripple, vibration and noise, particularly at low rotor speeds. However, as proved by Fig. 10, the cogging torque of the proposed 12-pole-rotor FMSR is rather low.

The output performances of the designed FMSRGs supplying an isolated, three-phase resistive load are computed using FE-based dynamic simulations. Fig. 11 shows the FE-computed dynamic electromagnetic torque developed by the 12-pole-rotor FMSR. The peak-to-peak value of dynamic torque ripple is less than 10% from rated torque. Smoothness of the developed electromagnetic torque depends on the selected number of rotor flux-barriers per pole and, consequently, on the size and placement of the embedded rotor-FMs (Zhang, 2015; Khan, 2010).

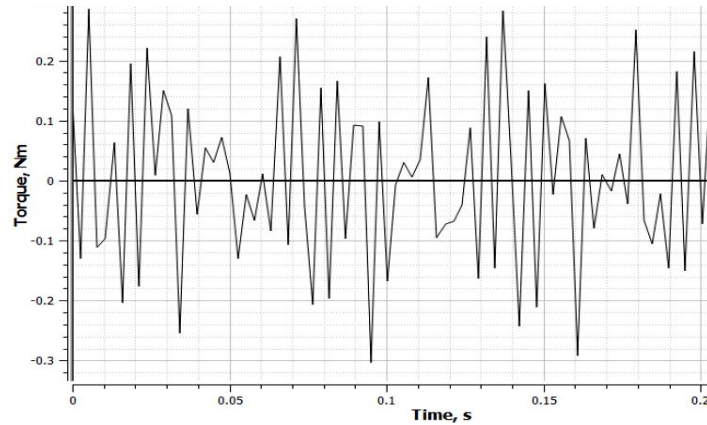


Fig. 10 – FE-computed cogging torque waveform for the proposed 12-pole-rotor FMSR.

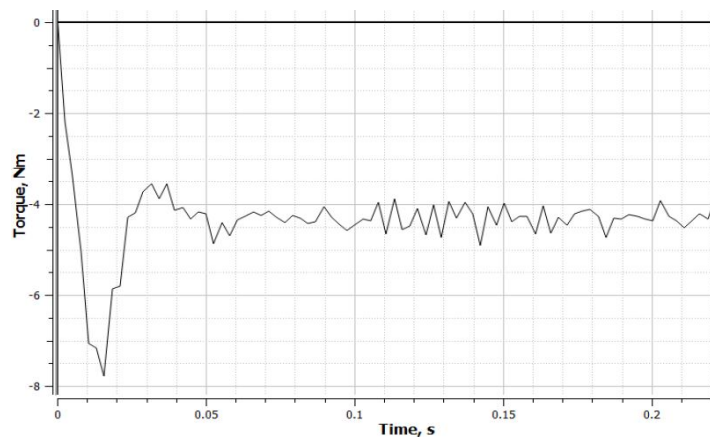
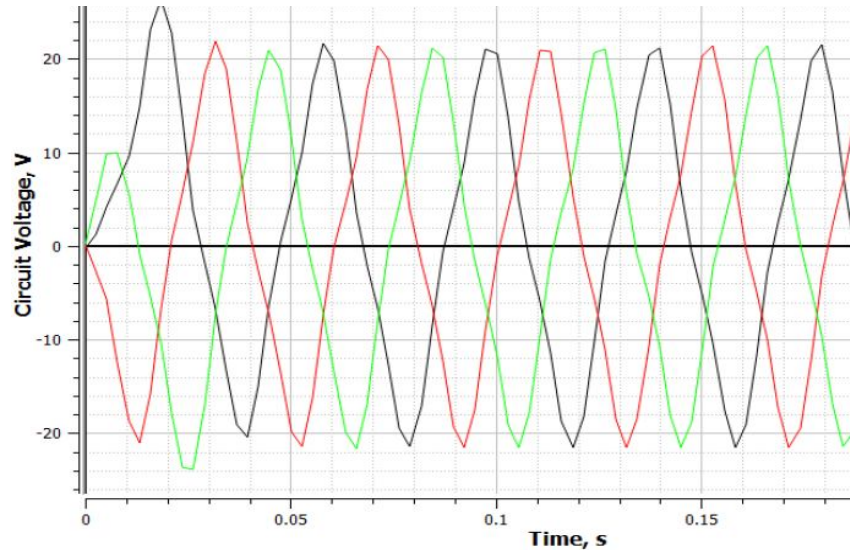
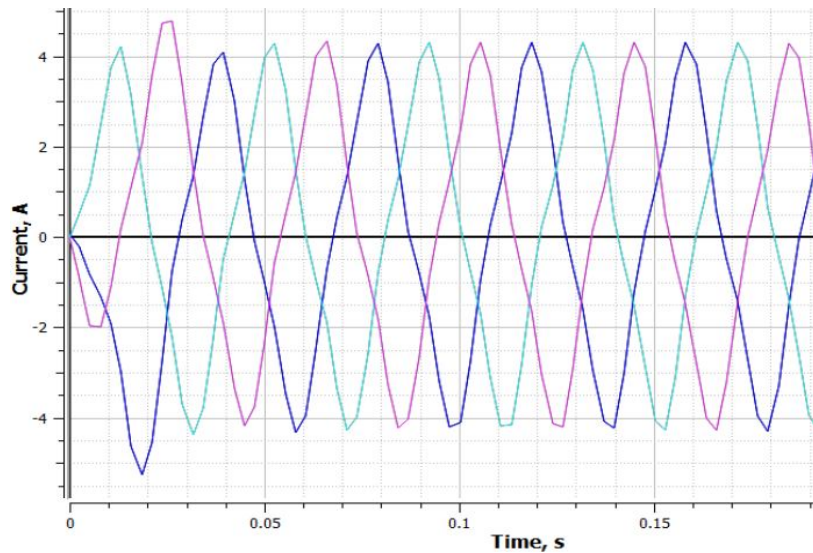


Fig. 11 – FE-computed dynamic electromagnetic torque developed under resistive-load operation of the proposed 12-pole-rotor FMSR.

FE-computed stator-winding phase-voltage and phase-current waveforms under resistive-load operation for the two FMASRGs are shown in Figs. 12 and 13, respectively. It is to be observed that the computed waveforms are quite sinusoidal for both FMASRG topologies.



a



b

Fig. 12 – FE-computed stator-winding phase-voltage (*a*) and phase-current (*b*) waveforms of the proposed 12-pole-rotor FMASRG operating under resistive load condition.

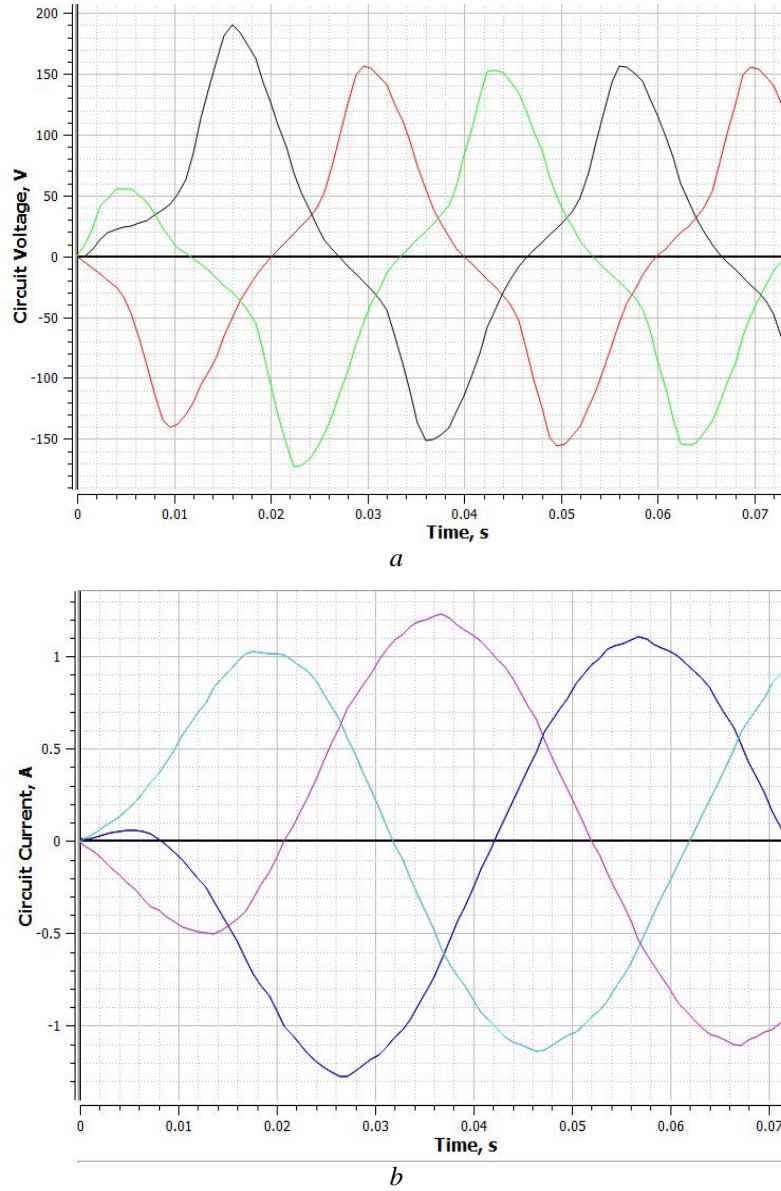


Fig. 13 – FE-computed stator-winding phase-voltage (*a*) and phase-current (*b*) waveforms of the proposed 8-pole-rotor FMSRSG operating under resistive load condition.

4. Conclusions

Multipolar designs of FMSRSG for stand-alone low-speed operation have been investigated in this paper. The proposed FMSRSG topologies entail

outer stator with conventional three-phase distributed winding, and inner rotor with low-cost FMs properly embedded in three-layer magnetic flux barriers.

FE-based magnetic field analyses and dynamic simulations carried out for evaluation of FMSRG designs and outer performances have shown that FMSRG is well suited for low-speed micro-wind power applications.

REFERENCES

- Baek J., Kwak S., Toliyat H. A., *Optimal Design and Performance Analysis of Permanent Magnet-Assisted Synchronous Reluctance Portable Generators*, J. Magn., South Korea, **18(1)**, 65-73 (2013).
- Boazzo B. *et al.*, *Multipolar Ferrite-Assisted Synchronous Reluctance Machines: A General Design Approach*, IEEE Trans. Ind. Electron., **62(2)**, 832-845 (2015).
- Fülöp H., Rădulescu M.M., Dranca M., *Design Analysis of Ferrite Magnet-Assisted Synchronous Reluctance Micro-Wind Generator*, 7th Internat. Conf. on Modern Power Systems – MPS 2017, 2017, Cluj-Napoca, Romania, 1-4.
- Khan K., Leksell M., Wallmark O., *Design Aspects on Magnet Placement in Permanent-Magnet Assisted Synchronous Reluctance Machines*, Proc. 5th IET Internat Conf. Power Electron. Mach. Drives – PEMD 2010, 2010, Brighton, UK.
- Prieto D., *Modélisation et optimisation des machines synchro- réluctantes à aimants permanents et de leur électronique*, Thèse de doctorat, École Supérieure d'Électricité (Supélec), Gif-sur-Yvette, 228 pp., 2015.
- Vagati A., Boazzo B., Guglielmi P., Pellegrino G., *Design of Ferrite-Assisted Synchronous Reluctance Machines Robust Toward Demagnetization*, IEEE Trans. Ind. Applicat., **50(3)**, 1768-1779 (2014).
- Zhang Z., Zhou L., *Design and Rotor Geometry Analysis of Permanent Magnet-Assisted Synchronous Reluctance Machines Using Ferrite Magnets*, J. Electr. Engng., **66(6)**, 311-316 (2015).

MAȘINA SINCRONĂ REACTIVĂ ASISTATĂ CU MAGNEȚI PERMANENȚI ÎN REGIM DE GENERATOR ELECTRIC

(Rezumat)

În lucrare sunt propuse două topologii de mașină sincronă reactivă asistată cu magneți permanenți de ferită pentru utilizare ca generatoare electrice cu acționare directă de la microturbine eoliene de viteze joase. Calculul electromagnetic de dimensionare se efectuează prin modelare analitică bazată pe schemele magnetice echivalente de circuit în axele d și q ale mașinii. Topologiile dimensionate preliminar sunt evaluate prin analiză numerică de câmp magnetic, iar performanțele lor, în regim de generator electric autonom, sunt estimate prin simulare dinamică.

